Available online at www.sciencedirect.com
ScienceDirect
Optics Communications 281 (2008) 1072–1076
OPTICS COMMUNICATIONS
www.elsevier.com/locate/optcom

A planar waveguide concave grating employing dielectric mirrors

Chun-Ting Lin [a,*], Yang-Tung Huang [b], Jung-Yaw Huang [a]

[a] Department of Photonics and Institute of Electro-Optical Engineering, National Chiao Tung University, Hsinchu 30010, Taiwan, ROC
[b] Department of Electronics Engineering and Institute of Electronics, National Chiao Tung University, Hsinchu 30010, Taiwan, ROC

Received 29 June 2007; received in revised form 11 October 2007; accepted 22 October 2007

Abstract

Dielectric mirrors, which yield high-reflectances on grating facets, are proposed for the design of a planar waveguide concave grating. The transfer-matrix method is used to derive an expression for the reflectance of a series of air slots and high-index stacks. The Full-WAVE software, a finite difference time-domain EM solver from R-Soft, is used to evaluate the loss of the resulting 2D waveguide grating. The simulation results show that the polarization-dependent loss (PDL) is below 0.25 dB when the proposed dielectric mirror is used. The influence of the width variation of the dielectric stack is also taken into account.

PACS: 42.25.Fx; 42.82.−m

Keywords: Planar waveguide; Concave grating; Dielectric mirror; Wavelength division multiplexing

1. Introduction

Planar waveguide demultiplexers/multiplexers, such as arrayed waveguide gratings (AWGs) and planar waveguide concave (etched) gratings, are of recent interest for the optical telecommunication systems due to their advantages of low insertion loss, low crosstalk, great potential for mass production, and high spectral resolution [3]. However, arrayed waveguide gratings encounter the inherent limits due to the larger die sizes, the lower free spectral range, and the higher sensitivity to environment perturbations. In contrast, the sizes of planar waveguide concave gratings can be smaller than those of AWGs because of the geometry of folded beams [6]. Concave gratings have been widely used in spectrographs [1–8] and narrow bandwidth lasers [9].

In this paper, a planar waveguide concave grating with a dielectric mirror is proposed to yield a high-reflectance and low polarization-dependent loss (PDL). Although metallization [10–13] can also be used to increase the reflectance of the grating, a metalized grating usually yields a higher PDL. This is particularly true in a Littrow mount [11]. To solve the problem, we show that a grating with facets employing dielectric mirrors can produce a high-reflectance bandwidth covering the entire C-band.

2. Transfer-matrix analysis

We first used the transfer-matrix method [14] to design a high-reflectance multi-slot stack. The E- and B-fields are continuous across the interfaces of the films. For the dielectric mirror design, a series of the air slots and the high-index stacks with the quarter-wave widths yield a desired high-reflectance. The fields at two outmost boundaries can be expressed in matrix form as

$$\begin{bmatrix} E_a \\ B_a \end{bmatrix} = R \begin{bmatrix} E_b \\ B_b \end{bmatrix}, \tag{1}$$

$$R = \begin{bmatrix} m_{11} & m_{12} \\ m_{21} & m_{22} \end{bmatrix} = R_1 R_2 R_3 \cdots R_n, \tag{2}$$

where E_a and B_a are the E- and B-fields at the input boundary, E_b and B_b denote the E- and B-fields at the output

* Corresponding author. Tel.: +886 3 5712121x54212; fax: +886 3 5724361.
E-mail address: rhino.eo91g@nctu.edu.tw (C.-T. Lin).

0030-4018/$ - see front matter © 2007 Elsevier B.V. All rights reserved.
doi:10.1016/j.optcom.2007.10.062

boundary. The overall transfer-matrix R is the product of all individual 2×2 transfer matrices. The individual 2×2 transfer-matrix R_j of the jth air slot or high-index stack can be expressed as [14]

$$R_j = \begin{bmatrix} \cos\delta_j & \frac{i\sin\delta_j}{\gamma_j} \\ i\gamma_j \sin\delta_j & \cos\delta_j \end{bmatrix}, \tag{3}$$

where δ_j denotes the phase difference due to one travel of the jth air slot or high-index stack and can be expressed as

$$\delta_j = k_0 \Delta_j = \left(\frac{2\pi}{\lambda_0}\right) n_j w_j \cos\theta_j. \tag{4}$$

For TE modes,

$$\gamma_j = n_j\sqrt{\epsilon_0\mu_0}\cos\theta_j; \tag{5}$$

for TM modes,

$$\gamma_j = n_j\sqrt{\epsilon_0\mu_0}/\cos\theta_j, \tag{6}$$

where k_0 denotes the propagation constant for the design wavelength λ_0, n_j, w_j, and θ_j denote the refractive index, the width, and the refractive angle of the jth air slot or high-index stack, respectively. The transmittance and the reflectance can be obtained as

$$T = \left|\frac{2\gamma_0}{\gamma_a m_{11} + \gamma_a\gamma_b m_{12} + m_{21} + \gamma_b m_{22}}\right|^2, \tag{7}$$

$$R = \left|\frac{\gamma_a m_{11} + \gamma_a\gamma_b m_{12} - m_{21} - \gamma_b m_{22}}{\gamma_a m_{11} + \gamma_a\gamma_b m_{12} + m_{21} + \gamma_b m_{22}}\right|^2, \tag{8}$$

where γ_a and γ_b denote the transmission constants for the input medium and the output medium. The width of the jth air slot or high-index stack, needed for the odd multiple m of quarter-wavelength, can be derived from (4) as

$$w_j = \frac{\Delta_j}{n_j\cos\theta_j} = \frac{m\cdot\frac{\lambda_0}{4}}{n_j\cos\theta_j}. \tag{9}$$

The side view of the slab waveguide structure with the proposed planar waveguide concave grating is shown in Fig. 1. The etched trenches form the air slots and the non-etched parts form the high-index stack for the dielectric mirror design. The slab waveguide consists of a 6 μm SiON core layer with the upper 6 μm and the lower 10 μm SiO_2 cladding layers grown on the silicon substrate. The refractive indices for the core layer, cladding layer, and the silicon substrate are 1.456, 1.450, and 3.476, respectively. The effective indices of TE_0 and TM_0 modes are 1.45393 and 1.45392, respectively. The slab waveguide supports the fundamental mode for both polarizations.

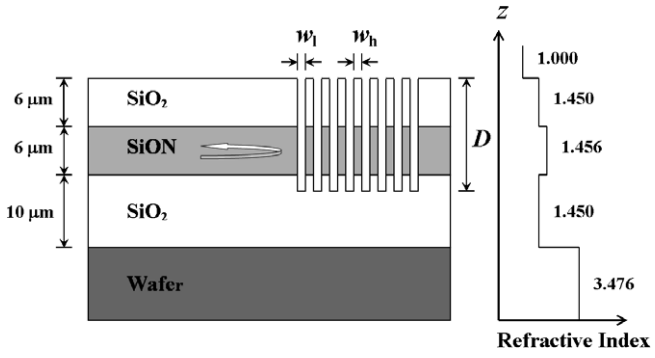

Fig. 1. Side view of the etched trenches for the dielectric mirror.

Fig. 2 shows the top view of a planar waveguide concave grating with dielectric mirrors. The entire C-band, covering from 1528.77 nm to 1560.61 nm, includes 81 wavelength channels with a channel spacing of 0.4 nm according to ITU grids [15]. The central wavelength is chosen to be 1544.69 nm. In the planar waveguide concave grating design, the blaze angle of the grating is chosen to make the incident angle of the light to be equal to the reflective angle of the light relative to the facet normal. In a Littrow mount, this leads to the light incident at normal incidence. From (5) and (6), the reflectances R for TE and TM modes are the same at normal incidence while they behave differently for oblique incidence.

In a Littrow mount with the air and high effective indices of 1 and 1.456, respectively, at a design wavelength λ_0 of 1544.69 nm and m of 11, the widths w_l and w_h of the air slot and the high-index stack can be calculated with (9) to be 4.25 μm and 2.92 μm, respectively. Simulation results show that the bandwidth of the high-reflectance region increases with the number N of the air slots increases as shown in Fig. 3. Here, the high-reflectance region is defined as the region of which the reflectance is higher than 95%. When the number N of the air slots is below 5, the reflectances of the wavelengths in the C-band are all below 95%, therefore the bandwidth of the high-reflectance region does not exist according to this definition.

For further analysis, the number N is chosen to be 15 and the calculated bandwidth of the high-reflectance region versus m in a Littrow mount are summarized in Table 1. By choosing $m = 11$ and $N = 15$, the reflectances R for TE and TM modes in a Littrow mount are shown in Fig. 4. Notice that the diffraction efficiency of a conventional metalized

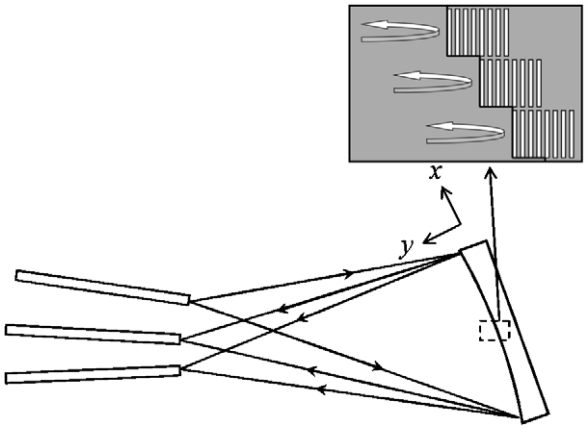

Fig. 2. Top view of a planar waveguide concave grating with dielectric mirrors.

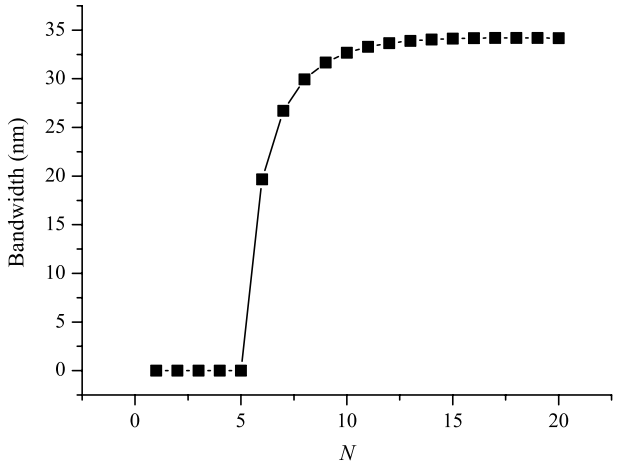

Fig. 3. Bandwidth versus N in a Littrow mount with m of 11 at a design wavelength λ_0 of 1544.69 nm.

Table 1
Bandwidth results of the high-reflectance region in a Littrow mount with N of 15 and λ_0 of 1544.69 nm

m	w_l (μm)	w_h (μm)	Range (nm)	Bandwidth (nm)
1	0.39	0.27	1377.26–1758.26	381.00
3	1.16	0.80	1484.79–1610.14	125.35
5	1.93	1.33	1508.28–1583.41	75.13
7	2.70	1.86	1518.58–1572.22	53.64
9	3.48	2.39	1524.36–1566.07	41.71
11	4.25	2.92	1528.06–1562.19	34.13
13	5.02	3.45	1530.63–1559.51	28.88
15	5.79	3.98	1532.52–1557.55	25.03
17	6.56	4.52	1533.97–1556.05	22.08
19	7.34	5.05	1535.12–1554.87	19.75

grating is polarization-dependent, originating from the induced surface current of the metal. The proposed grating employing a dielectric mirror with a dielectric-air interface therefore would be able to mitigate this undesired loss.

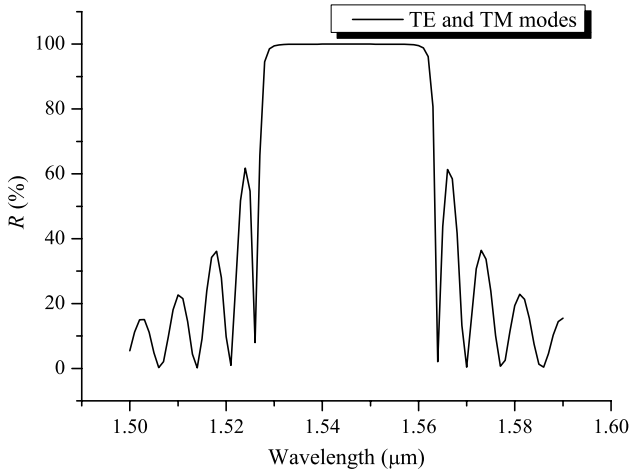

Fig. 4. Reflectances R for TE and TM modes versus the corresponding wavelength in a Littrow mount with m of 11 and N of 15 for the transfer-matrix analysis.

3. 2D waveguide analysis

For the analysis presented above, we assumed only the transverse fundamental mode along the z-axis is supported. To further evaluate the effect of etching depth on the reflectance and the bandwidth of the high-reflectance region, we further analyze the 2D waveguide with FullWAVE software from R-Soft. The waveguide structure of the etched trenches for one stack is coded into the software.

Fig. 5 shows the reflectance R versus the etched depth D in a Littrow mount with $m = 11$. We can see that almost no light is reflected by the mirror until the trench is etched to the core layer. Then the reflectance increases sharply and then saturates when the trench reaches to the lower cladding layer. The reflectance maintain stable when the etched depth is larger than 13 μm. Therefore, in our analysis the etched depth is chosen to be 13 μm. The waveguide is excited with the slab mode launched at the input, and the optical field is partially reflected by the dielectric mirror. The reflected field is analyzed with a time monitor positioned at the ending facet of the input medium. Most of light propagates in the core layer so the reflectance is low until the trench is etched through the core layer to reach the lower cladding layer.

Fig. 6 shows the reflectances of the TE and TM modes versus m in a Littrow mount with N of 15, D of 13 μm, and λ_0 of 1544.69 nm. Simulation results show that the reflectances for both modes decrease as m increases. The loss mainly comes from the scattering of light to the air when passing through the air slot. So when the width of the air slot increases with m, it leads to a deterioration of the reflectance. The PDL, defined as the difference between the diffraction efficiencies for the TE and TM modes, is 0.25 dB with m of 11, N of 15, and D of 13 μm. Fig. 7 shows the reflectance versus the corresponding wavelength in a Littrow mount with m of 11, N of 15, and D of 13 μm. Compared with the results obtained from the transfer-matrix method, the reflectance and the bandwidth of the high-reflectance region both decrease and the reflectances

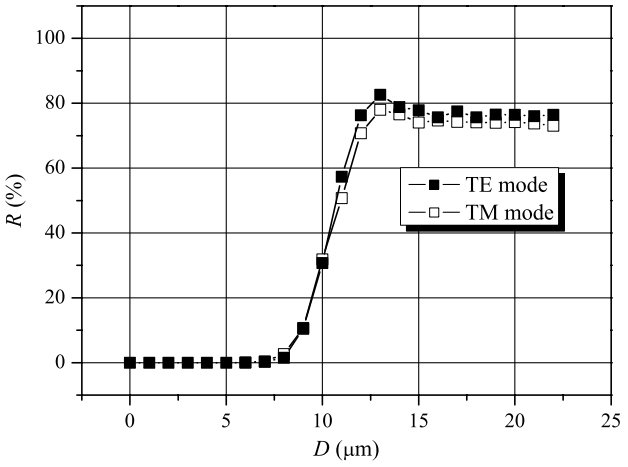

Fig. 5. Reflectance R versus D in a Littrow mount with m of 11 and N of 15 at a design wavelength λ_0 of 1544.69 nm.

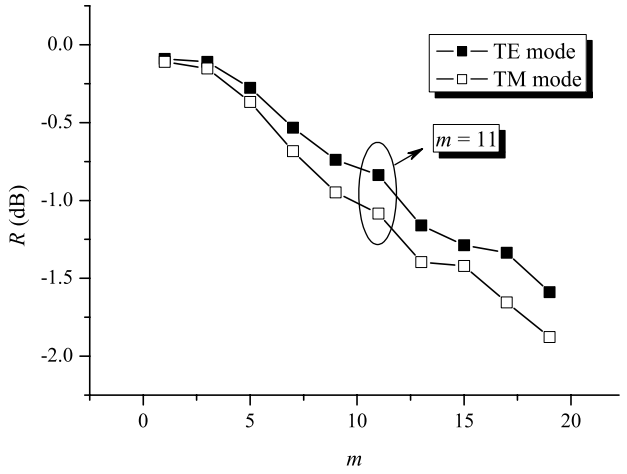

Fig. 6. Reflectance R versus m in a Littrow mount with N of 15 and D of 13 μm at a design wavelength λ_0 of 1544.69 nm.

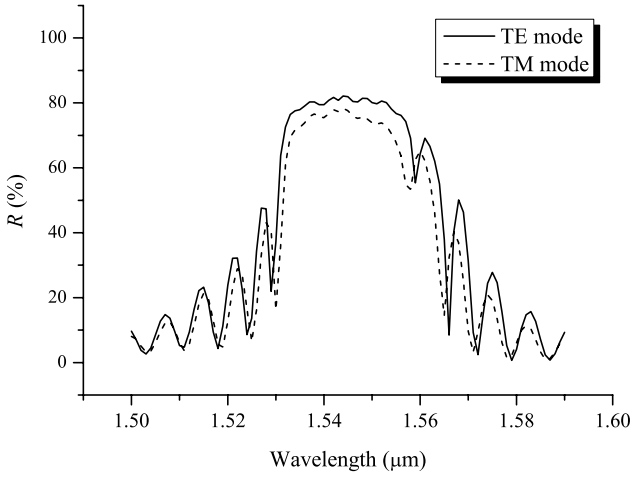

Fig. 7. Reflectance R versus the corresponding wavelength in a Littrow mount with m of 11, N of 15, and D of 13 μm for the 2 D waveguide analysis.

for the TE and TM modes are not identical in a Littrow mount. The reason is that the incident light used in the transfer-matrix analysis is the plane wave while optical beam profile used in the 2D waveguide analysis has a finite beam waist, which turns out to have a large influence on the reflectance.

For a conventional design, the metal coating on the shaded facet is the main source of the PDL especially in a Littrow mount [11]. The induced surface current does not exist in a dielectric-air interface and the dielectric mirror mitigates the effect of the PDL. However, the grating nonideality due to the width variation Δw of the air slot and the high-index stack during the fabrication process can significantly decrease the reflectance. The perturbed width w_l' and w_h' of the air slot and the high index stack can be expressed as

$$w_l' = w_l + \Delta w, \tag{10}$$

$$w_h' = w_h - \Delta w. \tag{11}$$

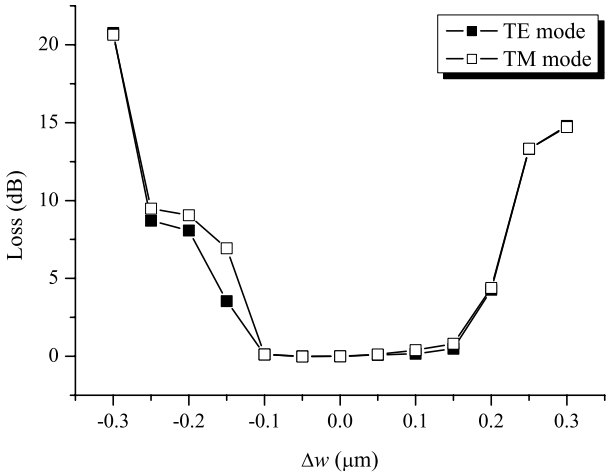

Fig. 8. Loss due to the width variation Δw in a Littrow mount with m of 11, N of 15, and D of 13 μm at a design wavelength λ_0 of 1544.69 nm.

Fig. 8 shows that the additional loss increases as the width variation increases. Simulation results show that when the width variation Δw is below ±0.1 μm the losses can be kept below 0.40 dB for both modes so the width variation below 0.1 μm is required to yield a dielectric mirror with high-reflectance.

4. Summary

In this paper, a planar waveguide concave grating employing dielectric mirrors is proposed to mitigate the PDL which comes from the induced surface current of the metal, especially in a Littrow mount. The transfer-matrix method is used to obtain the reflectance R and the number N of the air slots is chosen to be 15. Simulation results show that the reflectance is high for a wide range of the wavelength. The FullWAVE software from R-Soft is used to analyze the reflectance R for the 2D waveguide with etched air slots. Simulation results show that the PDL $\leqslant$ 0.25 dB can be achieved with m of 11, N of 15, and D of 13 μm. The impact of the fabrication error of etched air slots is also taken into account. To yield a proposed grating with high-reflectance, the width variation Δw should be below ±0.1 μm.

Acknowledgement

This work was supported in part by the National Science Council, Taiwan, ROC under the contract NSC 95-2221-E-009-250.

References

[1] H.W. Yen, H.R. Friedrich, R.J. Morrison, G.L. Tangonan, Opt. Lett. 6 (12) (1981) 639.
[2] Y. Fujii, J. Minowa, Appl. Opt. 22 (7) (1983) 974.
[3] E. Gini, W. Hunziker, H. Melchior, J. Lightwave Technol. 16 (4) (1998) 625.
[4] J.J. He, B. Lamontagne, A. Delâge, L. Erickson, M. Davies, E.S. Koteles, J. Lightwave Technol. 16 (4) (1998) 631.
[5] J. J He, IEEE J. Sel. Top. Quantum Electron. 8 (6) (2002) 1186.

[6] S. Janz, A. Balakrishnan, S. Charbonneau, P. Cheben, M. Cloutier, A. Delâge, K. Dossou, L. Erickson, M. Gao, P.A. Krug, B. Lamontagne, M. Packirisamy, M. Pearson, D.-X. Xu, IEEE Photon. Technol. Lett. 16 (2) (2004) 503.
[7] X. Chen, J.N. McMullin, C.J. Haugen, R.G. DeCorby, Opt. Commun. 237 (2004) 71.
[8] M. Ishikawa, T. Miura, A. Matsutani, F. Koyama, Jpn. J. Appl. Phys. 43 (8B) (2004) 5761.
[9] J.B.D. Soole, K.R. Poguntke, A. Scherer, H.P. Leblanc, C. Chang-Hasnain, J.R. Hayes, C. Caneau, R. Bhat, M.A. Koza, Appl. Phys. Lett. 61 (23) (1992) 2750.
[10] Z. Shi, J.J. He, S. He, J. Opt. Soc. Am. A 21 (7) (2004) 1198.
[11] Z. Shi, J.J. He, S. He, IEEE Photon. Technol. Lett. 16 (8) (2004) 1885.
[12] J. Song, J.J. He, S. He, IEEE J. Sel. Top. Quantum Electron. 11 (1) (2005) 224.
[13] J. Song, J.J. He, S. He, J. Opt. Soc. Am. A 22 (9) (2005) 1947.
[14] F.L. Pedrotti, L.S. Pedrotti, Introduction to Optics, Prentice Hall, New Jersey, 1993 (Chapter 19).
[15] S.V. Kartalopoulos, Introduction to DWDM Technology, IEEE, New York, 2000 (Chapter 15).